FIRST- AND SECOND-ORDER ADAPTIVE DIFFERENTIAL MICROPHONE ARRAYS

*Heinz Teutsch**

Telecommunications Laboratory
University of Erlangen-Nuremberg, Germany
Email address: teutsch@LNT.de

Gary W. Elko

Media Signal Processing Research Department
Agere Systems, Murray Hill, NJ, USA
Email address: gwe@agere.com

ABSTRACT

Whenever undesired noise sources are spatially non-stationary, conventional directional microphone technology has its limits in terms of interference suppression. Adaptive differential microphone arrays (ADMAs) with their null steering capabilities promise better performance. This contribution introduces and examines first- and second-order ADMAs based on fullband as well as on subband algorithms. A real-time implementation that demonstrates its usability is also presented.

1. INTRODUCTION

The presence of background noise accompanying all kinds of acoustic signal transmission is an ubiquitous problem. Speech signals in particular suffer from incident background noise. Undesired signals, such as background noise, can make conversations in adverse acoustic environments virtually impossible without applying appropriately designed electroacoustic transducers and sophisticated signal processing.

The utilization of conventional directional microphones with fixed directivity is a limited solution to this problem because the undesired noise is often not fixed to a certain angle. A better approach to solving this problem is to take advantage of the adaptive noise cancellation capabilities of differential microphone arrays in combination with digital signal processing.

This paper discusses first- and second-order ADMAs which are able to adaptively track and attenuate possibly moving noise sources that are located in the back half plane of the array. This noise attenuation is achieved by adaptively placing a null into the jammer's direction of arrival. Section 2 and Section 3 present the theory underlying first- and second-order ADMAs based on a fullband approach. Section 4 extends these ideas to a subband based algorithm. Section 5 briefly describes a real-time implementation running under the Microsoft® Windows® operating system as well as measurement results.

2. FIRST-ORDER FULLBAND ADMA

The magnitude of the frequency and angular dependent response of a first-order differential array for a signal point source at a distance where farfield conditions are applicable (see Fig. 1) can be written as

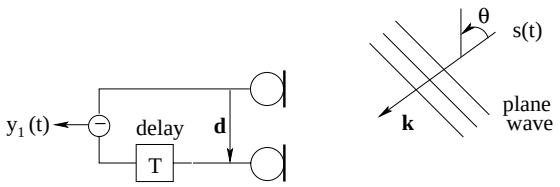

***Figure 1*:** *First-order differential microphone array*

$$|H_1(f,\theta)| = \left|\frac{Y_1(f,\theta)}{S(f)}\right| = \left|1 - e^{-j(2\pi f T + \mathbf{k}\cdot\mathbf{d})}\right| = 2\sin\frac{2\pi f\big[T + (d\cos\theta)/c\big]}{2}, \quad (1)$$

where $S(f)$ is the spectrum of the signal source, $|\mathbf{k}| = k = 2\pi f/c$ is the wavenumber, c is the speed of sound and $\mathbf{d}$ is the displacement vector. For small element spacing and inter-element delay ($kd \ll \pi$ and $T \ll 1/2f$) Eq. 1 can be approximated as

$$|H_1(f,\theta)| \approx 2\pi f\big[T + (d\cos\theta)/c\big]. \quad (2)$$

As can be seen, Eq. (2) consists of a monopole term and a dipole term ($\cos\theta$). Note that the amplitude response of the first-order differential array rises linearly with frequency. This frequency dependence can be easily corrected for by applying a first-order lowpass filter at the array output. The directivity response can then be expressed by

$$D_1(\theta) = \frac{T}{T + d/c} + \left(1 - \frac{T}{T + d/c}\right)\cos\theta. \quad (3)$$

It is obvious that an implementation of a first-order ADMA would require the ability to generating *any* time delay T between the two microphones. Obviously, this approach is not suitable for a real-time system.

A way to circumvent the necessity to generate the delay T directly in order to obtain the desired directivity response is to utilize an adaptive back-to-back cardioid system as shown in Fig. 2. This system can be used to adaptively adjust the response of the backward facing cardioid (see Fig. 3) in order to track a possibly moving noise source in the back half plane. By choosing $T = d/c$, the back-to-back cardioid can be formed directly by appropriately subtracting the delayed microphone signals.

It can be shown that the transfer function of the first-

* This work was performed at the Media Signal Processing Research Department, Agere Systems, Murray Hill , NJ, USA

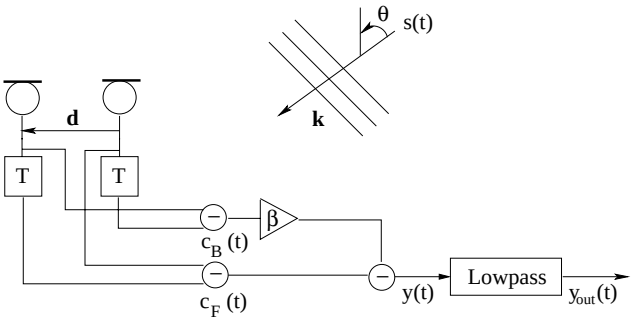

***Figure 2*:** *First-order fullband ADMA*

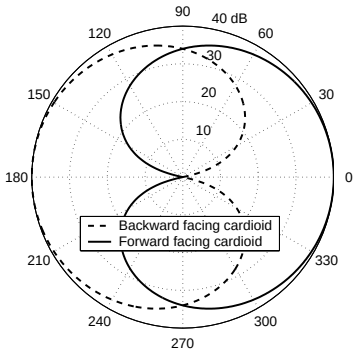

***Figure 3*:** *Directivity pattern of the first-order back-to-back cardioid system*

order ADMA can be written as

$$H_1(f,\theta) = \frac{Y_{out}(f,\theta)}{S(f)} = 2j\, e^{-j\pi fT} \cdot\left(\sin\frac{kd(1+\cos\theta)}{2} - \beta\sin\frac{kd(1-\cos\theta)}{2}\right). \quad (4)$$

The single independent null angle θ_1 of the first-order ADMA, which in this work is assumed to be placed into the back half plane of the array ($90^\circ \leq \theta_1 \leq 180^\circ$), can be found by setting Eq. (4) to zero and solving for $\theta = \theta_1$. Therefore,

$$\theta_1 = \arccos\left(\frac{2}{kd}\arctan\left(\frac{\beta-1}{\beta+1}\ \tan\frac{kd}{2}\right)\right), \quad (5)$$

which for small spacing and delay can be approximated as

$$\theta_1 \approx \arccos\frac{\beta-1}{\beta+1}, \quad (6)$$

where $0 \leq \beta \leq 1$ under the constraint $90^\circ \leq \theta_1 \leq 180^\circ$. A selection of directivity patterns that can be obtained by an first-order ADMA is depicted in Fig. 4.

In a time-varying environment, it is advisory to use an adaptive algorithm in order to obtain the update of the parameter β. For this matter, the normalized least-mean-square (NLMS) adaptive algorithm is utilized, which is computationally inexpensive, easy to implement and which offers reasonably fast tracking capabilities. Here, the real valued time-domain one-tap NLMS algorithm can be written as

$$y(i) = c_{\mathrm{F}}(i) - \beta(i)c_{\mathrm{B}}(i), \quad (7a)$$

$$\beta(i+1) = \beta(i) + \frac{\mu}{a + ||c_{\mathrm{B}}(i)||^2}c_{\mathrm{B}}(i)y(i), \quad (7b)$$

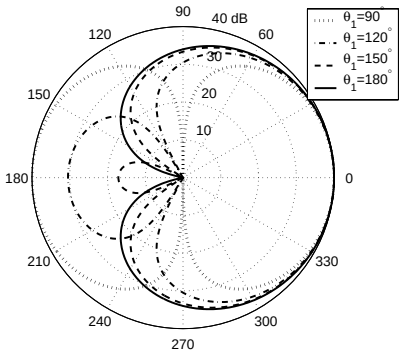

***Figure 4*:** *Various directivity patterns for a first-order ADMA*

where $c_{\mathrm{F}}(i)$ and $c_{\mathrm{B}}(i)$ are the values for the forward and the backward facing cardioid signals at time instance i, $0 < \mu < 2$ is the adaptation constant and $a > 0$ is a small constant.

3. SECOND-ORDER FULLBAND ADMA

By combining two first-order differential arrays as shown in Fig. 1, and after introducing an additional time delay T_2, a general second-order differential microphone array can be constructed as shown in Fig. 5.

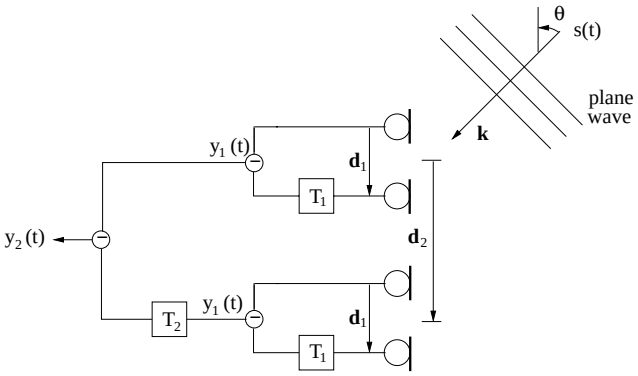

***Figure 5*:** *Second-order differential microphone array*

After examining Fig. 5 it can be readily shown that the magnitude of the frequency and angular dependent response of a second-order differential farfield array reads

$$|H_2(f,\theta)| = \left|\frac{Y_2(f,\theta)}{S(f)}\right| = 4\prod_{\nu=1}^{2}\sin\frac{2\pi f\big[T_\nu + (d_\nu\cos\theta)/c\big]}{2}, \quad (8)$$

which, for the special case of small spacing and delay, i.e. $kd_1, kd_2 \ll \pi$ and $T_1, T_2 \ll 1/2f$, becomes

$$|H_2(f,\theta)| \approx (2\pi f)^2\prod_{\nu=1}^{2}\big[T_\nu + (d_\nu\cos\theta)/c\big]. \quad (9)$$

As in the case of the first-order differential array, the amplitude response of the second-order array consists of a monopole term and a dipole term ($\cos\theta$) and an additional quadrupole term ($\cos^2\theta$). Also, a quadratic rise as a function of frequency can be observed. This frequency dependence can be easily equalized by applying a second-order

lowpass filter. The directivity response can then be expressed by

$$D_2(\theta) = \prod_{\nu=1}^{2} \left(\frac{T_\nu}{T_\nu + d_\nu/c} + \left(1 - \frac{T_\nu}{T_\nu + d_\nu/c}\right) \cos\theta \right), \quad (10)$$

which is a direct result of the pattern multiplication theorem in electroacoustics.

One design goal of the second-order differential farfield array was to be able to use the array in a host-based environment without the need for any special purpose hardware, e.g. additional external DSP interface boards. Therefore, two dipole elements are utilized in order to form the second-order array instead of four omnidirectional elements. As a consequence, $T_1 \equiv 0$ which means that one null angle is fixed to $\theta_{21} = 90^\circ$. In other words, although two independent nulls can be formed by the second-order differential array, only one can be made adaptive if two dipole elements instead of four omnidirectional transducers are used. On the other hand, the implementation of a second-order ADMA is identical to the first-order ADMA as shown in Fig. 2 if $\mathbf{d} = \mathbf{d}_2$, $T = T_2$, $\beta = \beta_2$ and d_1 is the acoustical dipole length of the dipole transducer. Additionally, the lowpass is chosen to be a second-order lowpass filter. The second-order back-to-back cardioid system, which again can be obtained by appropriately subtracting the delayed microphone signals, is shown in Fig. 6.

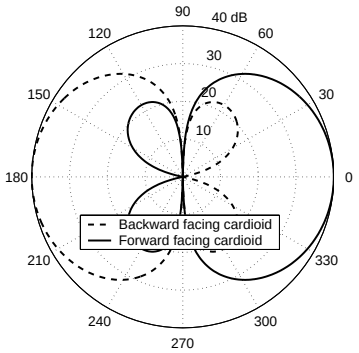

Figure 6: *Directivity pattern of the second-order back-to-back cardioid system*

Considering the modified block diagram (Fig. 2) it can be easily verified that the transfer function of the second-order ADMA can be written as

$$H_2(f,\theta) = \frac{Y_{out}(f,\theta)}{S(f)} = -4\, e^{-j\pi f T_2} \sin\left(\frac{kd_1 \cos\theta}{2}\right) \cdot \left(\sin\frac{kd_2(1+\cos\theta)}{2} - \beta_2 \sin\frac{kd_2(1-\cos\theta)}{2} \right), \quad (11)$$

and it follows for the null angles

$$\theta_{21} = 90^\circ, \quad (12a)$$

$$\theta_{22} \approx \arccos\frac{\beta_2 - 1}{\beta_2 + 1}, \quad (12b)$$

where $0 \le \beta_2 \le 1$ under the constraint $90^\circ \le \theta_{22} \le 180^\circ$. A selection of directivity patterns that can be obtained by a second-order ADMA consisting of two dipole elements are depicted in Fig. 7.

As shown in [1], the second-order differential array is superior to the first-order differential array in terms of directivity index, front-to-back ratio and beamwidth.

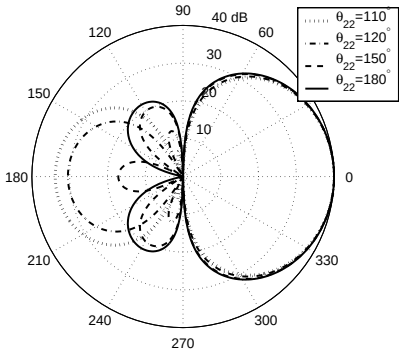

Figure 7: *Various directivity patterns for a second-order ADMA*

4. SUBBAND ADMA

One additional degree of freedom can be obtained by performing the adaptive algorithm in subbands. Figure 8 depicts a subband two-element ADMA, where the two elements can be either omnidirectional (first-order ADMA) or dipole (second-order ADMA) elements.

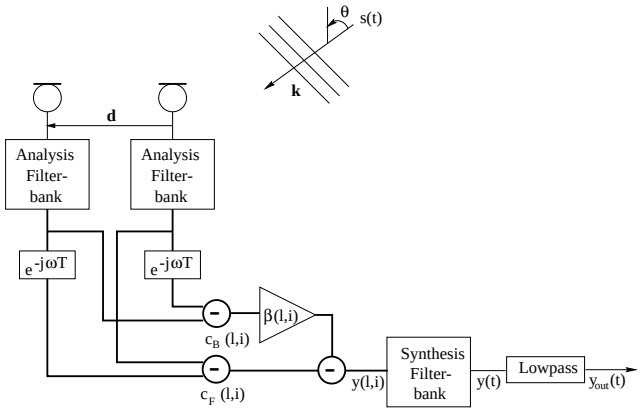

Figure 8: *A subband two-element ADMA*

The parameter $\beta(l,i)$, where l denotes the subband bin and i is the discrete time instance, is updated by an adaptive algorithm that minimizes the output power of the array. This update therefore effectively adjusts the response of the backward-facing cardioid $c_B(l,i)$ and can be written as

$$y(l,i) = c_F(l,i) - \beta(l,i) c_B(l,i), \quad (13a)$$

$$\tilde{\beta}(l,i+1) = \beta(l,i) + \frac{\mu y(l,i) c_B(l,i)}{||c_B(l,i)||^2 + a}, \quad (13b)$$

where

$$\beta(l,i) = \begin{cases} \tilde{\beta}(l,i), & 0 \le \tilde{\beta}(l,i) \le 1 \\ 0, & \tilde{\beta}(l,i) < 0 \\ 1, & \tilde{\beta}(l,i) > 1 \end{cases}, \quad (14)$$

and μ is the update parameter and a is a positive constant.

By using this algorithm, multiple spatially distinct noise sources with non-overlapping spectra located in the back half plane of the ADMA can be tracked and attenuated simultaneously.

5. IMPLEMENTATION AND MEASUREMENTS

A PC-based real-time implementation running under the Microsoft® Windows® operating system was realized using a standard soundcard as the analog-to-digital converter. Two omnidirectional elements of the type Panasonic WM-54B as well as two dipole elements of the type Panasonic WM-55D103 and a microphone preamplifier offering 40 dB gain comprise the analog front-end.

The easiest way to obtain the signals for the forward facing cardioids $c_{\mathrm{F}}(t)$ and the backward facing cardioids $c_{\mathrm{B}}(t)$ as shown in Fig. 2 and Fig. 8 is to choose the spacing between the microphones such that there is exactly one sample delay between the delayed and the undelayed microphone signals. Therefore, the sampling frequency was set to $f_s = 22050$ Hz with $d = d_2 = 1.54$ cm. For the dipole elements, the acoustical dipole length d_1 was found to be 0.8 cm.

It is difficult to reproduce the tracking capabilities of the ADMAs here but static directivity patterns for various setups can be shown. Fig. 9 depicts the fullband ADMA directivity pattern for both first-order and second-order array. These measurements were performed by placing a broadband jammer at approximately 90° with respect to the array's axis utilizing a standard directivity measurement technique. It can be seen that deep nulls covering a wide frequency range are formed in the direction of the jammer.

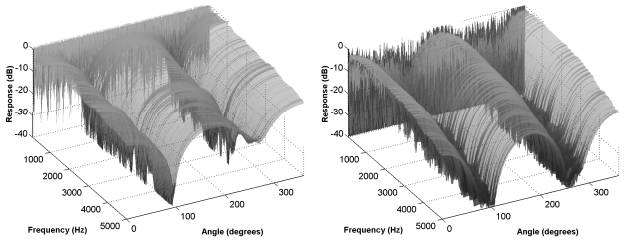

***Figure 9*:** *Measured fullband ADMA directivity for a broadband jammer incident at $\theta_1 = \theta_{22} = 90^\circ$ (left: first-order ADMA, right: second-order ADMA)*

Similar measurements were performed for the subband ADMAs which are reproduced in Figs. 10 and 11. Here, four loudspeakers simultaneously playing sinusoidal signals were positioned in the back half plane of the arrays at the approximate positions indicated in Figs. 10 and 11. As can be seen, these measurements are in close agreement with the simulated patterns as shown in Figs. 4 and 7.

In order to combat the noise amplification properties inherent in differential arrays, a noise reduction method as presented in [2] has been beneficially included in the demonstrator.

Using the same set of hardware, a nearfield mode of operation where the array can be utilized in close-talking applications with imperfect sensor placement has also been examined, implemented (see [3]) and incorporated into the demonstrator.

6. CONCLUSIONS

First- and second-order ADMAs which are able to adaptively track and attenuate a possibly moving noise source located in the back half plane of the arrays have been presented. It has been shown that by performing the calculations in subbands even multiple spatially distinct noise sources with non-overlapping spectra can be tracked and attenuated simultaneously. The real-time implementation presents the dynamic performance of the ADMAs in real acoustic environments and shows the practicability of using these arrays as acoustic front-ends for a variety of applications including telephony, automatic speech recognition and teleconferencing.

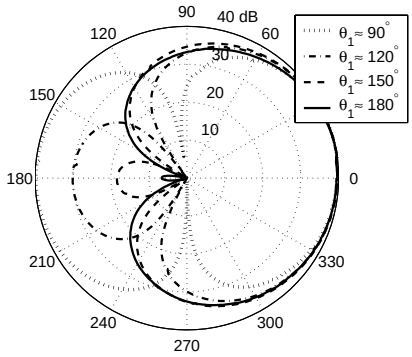

***Figure 10*:** *Measured first-order subband ADMA directivity for four simultaneously playing sinusoids*

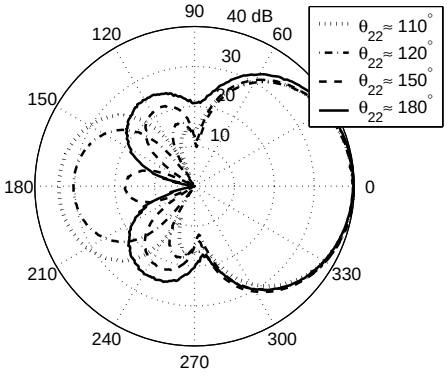

***Figure 11*:** *Measured second-order subband ADMA directivity for four simultaneously playing sinusoids*

7. REFERENCES

[1] Elko, G. W.: *Superdirectional Microphone Arrays.* In J. Benesty and S. L. Gay (eds.),'Acoustic Signal Processing for Telecommunication', pp. 181-236, Kluwer Academic Publishers, 2000.

[2] Diethorn, E. J.: *A Subband Noise-Reduction Method for Enhancing Speech in Telephony & Teleconferencing.* IEEE Workshop on Applications of Signal Processing to Audio and Acoustics, Mohonk, USA, 1997.

[3] Teutsch, H. and Elko, G. W.: *An Adaptive Close-Talking Microphone Array.* IEEE Workshop on Applications of Signal Processing to Audio and Acoustics, Mohonk, USA, 2001.

[4] Haykin, S.: *Adaptive Filter Theory.* Third ed., Prentice Hall, Englewood Cliffs, NJ, USA, 1996.